

Spin Excitation in d -wave Superconductors : A Fermi Liquid Picture

Khee-Kyun Voo, Hong-Yi Chen, and W. C. Wu

Department of Physics, National Taiwan University, Taipei 11650, Taiwan, R.O.C.

(November 13, 2018)

A detailed study of the Inelastic Neutron Scattering (INS) spectra of the high- T_c cuprates based on the Fermi liquid (FL) picture is given. We focus on the issue of the transformation between the commensurate and incommensurate (IC) excitation driven by frequency or *temperature*. For $\text{La}_{2-x}\text{Sr}_x\text{CuO}_4$ (LSCO), the condition of small $\Delta(0)/v_F a$ (where a is the lattice constant, and henceforth will be set to 1) can simultaneously reproduces the always existing IC peaks in the superconducting (SC) and normal state, and the always fixed location at temperature or frequency change. For $\text{YBa}_2\text{Cu}_3\text{O}_{6+x}$ (YBCO), a moderate $\Delta(0)/v_F a$ and proximity of the van Hove singularity (vHS) at $\bar{M} = (0, \pi)$ to the Fermi level can reproduce the frequency- and temperature-driven shifting IC peaks in the SC state, and the vanishing of the IC peak in the normal state. The commensurate peak is found to be more appropriately described as a random phase approximation (RPA) effect. We address the conditional peak shifting behavior to a refined consideration on the nesting effect which is previously overlook. As a result, both the data on LSCO and the recent data on YBCO (on $\text{YBa}_2\text{Cu}_3\text{O}_{6.7}$ by Arai *et al.* and $\text{YBa}_2\text{Cu}_3\text{O}_{6.85}$ by Bourges *et al.*) can be reasonably reconciled within a FL picture. We also point out that the one-dimensional-like data by Mook *et al.* on a detwinned and more underdoped sample $\text{YBa}_2\text{Cu}_3\text{O}_{6.6}$ could be due to a gap anisotropy effect discussed by Rendell and Carbotte, and we proceed to suggest a way of clarifying it.

PACS numbers: 78.30.-j, 74.62.Dh, 74.25.Gz

I. INTRODUCTION

The aim of this paper is twofold. The first is to give a comprehensive study of the essential properties of the BCS spin susceptibility, both bare and RPA-corrected. The second, basing on the simplest RPA theory we account for the present strongly contrasting INS data on LSCO [1] and YBCO [2,3].

Magnetic fluctuation in the high- T_c cuprates has been long believed to be very intimately related to their superconductivity mechanism. Therefore various kinds of magnetic measurements such as Nuclear Magnetic Resonance (NMR), Nuclear Quadrupole Resonance (NQR), and INS have been carried out on the system, and aimed for clarifying the connection between the two. Among those measurements, INS experiments is the one which distinguishes itself from others by its capability to measure the fluctuation locally in momentum and frequency space and hence making itself an indispensable and important tool. Especially recently it provides a great deal of new observations, which has yet reached a consensus.

Essentially there are two dominant features of the observed INS spectra, the existence of commensurate peak at $\mathbf{Q}_{AF} \equiv (\pi, \pi)$, and IC peak at $\mathbf{Q}_\delta \equiv (\pi, \pi \pm \delta)$ and $(\pi \pm \delta, \pi)$. The spectra in LSCO [4,1,5] is always IC and have a incommensurability independent of ω and T but increases with hole-doping. On the other hand, YBCO [3,2,6] and $\text{Bi}_2\text{Sr}_2\text{CaCu}_2\text{O}_{8+x}$ (BSCCO) [7,8] compounds exhibit both commensurate and IC peaks. Very recently a comprehensive INS data on YBCO is obtained [3,2]. In the low-temperature SC state, it shows a commensurate

peak at a particular frequency $\omega_o(T = 0)$. Departing from ω_o (either go below or above ω_o), the peak is split up into IC and the incommensurability is continuously increased. The IC peak is found to appear only above some threshold frequency. In the normal state, the excitation is always a broad commensurate or weakly IC structure. At rising temperature to T_c , the incommensurability of the low frequency IC structure at low temperature is continuously closed up to commensurate. Such behavior is seen in an underdoped [2] and nearly optimally doped YBCO [3] (while YBCO data on a broad doping range are not available). These behaviors are in strong contrast to LSCO, and therefore raise an important question as whether the INS spectra in YBCO and LSCO are of the same origin.

There are also reports of the observation of the commensurate resonance in the pseudo-gap phase of underdoped YBCO at the same frequency as in the SC phase. But that remains controversial [9]. At all doping levels, its resonance nature is only well-established in the SC phase.

Perhaps the most straightforward and simplest interpretation of the IC peak is the Fermi surface (FS) nesting effect (see e.g., Ref. [10–14] and references therein). Many of the theoretical approaches assume that the system is spatially homogeneous and ultimately end up at a FS, could it be a FS of conventional electrons or a FS of some exotic fermion such as the spinon. The spin excitation is constituted by those low energy excitations nearby the Fermi surface. Such scenarios are capable of producing frequency-shifted IC peaks [10–12], and furthermore,

the commensurate peak is easily derived either from the bare or RPA susceptibility.

The Stripe ordering picture [15] is an alternative which predicts fixed IC peaks in spin and charge excitations that have incommensurability directly proportional to, and depending only on doping. In this picture the system is segregated into one-dimensional hole-rich stripes in which the holes can freely move, and electron-rich stripes in which electrons are ordered antiferromagnetically. The electron filling determines the length scale and thus the incommensurability. It is believed that the static stripe at the 1/8-doping [16], and the 2-to-1-coupled charge and spin excitations [17] are observed. That has boosted a lot of works on the “dynamic” stripe which also aims at the connection with the superconductivity mechanism. A plain Stripe model predicts no commensurate peak.

Therefore the Stripe picture seems to work well in LSCO, while the FL picture works well in YBCO. This is intriguing if one adheres to the philosophy that they all belong to the cuprate family and therefore should lay in a single unified theory. Here we argue that the discrepancies could be reconciled if the problem is considered more carefully. The frequency and temperature driven peak shifting present in YBCO but not in LSCO can be accounted for by a flatter electronic dispersion near FS such that the excitation can be scattered farther from it, while electronic dispersion of LSCO is far more steep near FS. A refined consideration of the nesting effect, which we have termed the *dynamic local nesting* effect is important when the condition $\Delta/v_F \ll \pi$ is violated. In the regime of having shifting IC peak in SC state, the IC peak is necessarily vanishes in the normal state. The commensurate resonance in the SC state of YBCO and BSCCO is addressed as a consequence of the experimentally observed closeness of the vHS at \bar{M} to the Fermi level [18–22]. The effect of the band singularity has been shown in many cases to be significant, such as providing the vanishing isotope effect, transport anomalies, high SC transition temperature, and so on. In short, we have argued that the apparently contradictory INS data can have a common basis in the FL regime.

We should also mention the data of Mook *et al.* [23] on a detwinned and more underdoped YBCO, $\text{YBa}_2\text{Cu}_3\text{O}_{6.6}$. The one-dimensional nature of the data where the IC peaks are found only along one of the crystal axis, is claimed by the authors as a strong evidence of stripe’s existence. Nevertheless we point out in Sec. VII that such behaviors can be due to an anisotropy effect in the FL picture. The effect is prominent in the frequency regime where the data in Ref. [23] was taken.

This study is also important in the aspect that it provides a comprehensive and detailed survey of the major consequences from the FL picture, and thus acts as a reference to see how much of the experimentally observed behaviors are really deviating from it. Comparisons with experiments are made where possible.

Our discussion will be focused on the evolution of the peak intensity and location in the parameter space of ω

and T . We organize this paper into sections and a brief summary of the findings of each sections or subsections is given at their ends where necessary. The first several sections are focused on the effect of dispersion v_F on the IC excitation. Sec. II gives the formalism and explains how the dispersion at Fermi level v_F is modeled. Sec. III gives the bare spectra in SC state, normal state, and at the transition. Sec. IV discusses the underlying machinery of the formation and behaviors of the IC peaks. Sec. V studies the effect of inclusion of the Hubbard repulsion or AF interaction into the system via RPA. An appropriate description of LSCO is given. Sec. VI is devoted to the relation between the INS peaks (commensurate and incommensurate) and \bar{M} -point vHS. An appropriate description of YBCO is then given. Sec. VII is a discussion on the anisotropy effect and the one-dimensional nature in INS spectrum. Finally, Sec. VIII gives a discussion of the results and conclusions.

II. FORMALISM

What we need in a FL description of the INS spectrum is the existence of a well-defined FS and the dispersion nearby. All low energy processes are constituted by the excitation at the vicinity of the Fermi surface.

A INS spectrum is proportional to $\text{Im}\chi(\mathbf{q}, \omega)$ besides some Bose-Einstein distribution factor due to the bosonic character of the excitation. Here $\chi(\mathbf{q}, \omega)$ is the spin susceptibility. The BCS bare spin susceptibility is given below and followed by the RPA-corrected susceptibility.

The BCS bare spin susceptibility in a one-layer SC system (the susceptibility in a normal system could be obtained by letting $\Delta \rightarrow 0$) is

$$\begin{aligned} \chi_o(\mathbf{q}, \omega) = & -\frac{1}{4} \sum_{\mathbf{k}} \left[\left[1 - \frac{\xi_{\mathbf{k}}\xi_{\mathbf{k}+\mathbf{q}} + \Delta_{\mathbf{k}}\Delta_{\mathbf{k}+\mathbf{q}}}{E_{\mathbf{k}}E_{\mathbf{k}+\mathbf{q}}} \right] \right. \\ & \times \left[\frac{1 - f(E_{\mathbf{k}}) - f(E_{\mathbf{k}+\mathbf{q}})}{\omega - E_{\mathbf{k}} - E_{\mathbf{k}+\mathbf{q}} + i\Gamma} - \frac{1 - f(E_{\mathbf{k}}) - f(E_{\mathbf{k}+\mathbf{q}})}{\omega + E_{\mathbf{k}} + E_{\mathbf{k}+\mathbf{q}} + i\Gamma} \right] \\ & - \left[1 + \frac{\xi_{\mathbf{k}}\xi_{\mathbf{k}+\mathbf{q}} + \Delta_{\mathbf{k}}\Delta_{\mathbf{k}+\mathbf{q}}}{E_{\mathbf{k}}E_{\mathbf{k}+\mathbf{q}}} \right] \\ & \times \left. \left[\frac{f(E_{\mathbf{k}}) - f(E_{\mathbf{k}+\mathbf{q}})}{\omega - E_{\mathbf{k}} + E_{\mathbf{k}+\mathbf{q}} + i\Gamma} - \frac{f(E_{\mathbf{k}}) - f(E_{\mathbf{k}+\mathbf{q}})}{\omega + E_{\mathbf{k}} - E_{\mathbf{k}+\mathbf{q}} + i\Gamma} \right] \right], \quad (1) \end{aligned}$$

where \mathbf{q} and ω are respectively the momentum and energy transfers. $f(E_{\mathbf{k}})$ is the Fermi function and $E_{\mathbf{k}} = (\xi_{\mathbf{k}}^2 + \Delta_{\mathbf{k}}^2)^{1/2}$ is the quasiparticle spectrum with $\xi_{\mathbf{k}}$ and $\Delta_{\mathbf{k}}$ the band dispersion and SC gap respectively. Henceforth we will write $\chi'_o \equiv \text{Re}\chi_o$, $\chi''_o \equiv \text{Im}\chi_o$, and likewise for χ in Eq. (3).

We use a two-dimensional tight-binding electronic dispersion

$$\xi_{\mathbf{k}} = -2t(\cos k_x + \cos k_y) - 4t' \cos k_x \cos k_y - \mu, \quad (2)$$

where t and t' are the nearest-neighbor (NN) and next-nearest-neighbor (NNN) hopping respectively. μ is the

chemical potential. In this paper only the $d_{x^2-y^2}$ -gap is treated (except in Sec. VII) since it is meant to describe the high- T_c cuprates. It is taken as $\Delta_{\mathbf{k}} = \Delta(T)(\cos k_x - \cos k_y)/2$. The width Γ/t in numerical integration is taken within $0.002 \sim 0.008$ with slicing 2000×2000 or 4000×4000 .

Equation (1) describes two kinds of excitation, the pair-breaking excitation that excites two quasiparticles from the SC condensate and costs energy $E_{\mathbf{k}} + E_{\mathbf{k}+\mathbf{q}}$, and the thermal one-particle excitation that excites a quasiparticle from $\mathbf{k} + \mathbf{q}$ to \mathbf{k} which costs energy $E_{\mathbf{k}} - E_{\mathbf{k}+\mathbf{q}}$. The two-particle excitation vanishes in the normal state while the one-particle excitation vanishes at zero-temperature SC state.

Here we want to make several important remarks on the modeling [by the simple dispersion Eq. (2)] of the dispersion gradient at FS (Fermi velocity v_F) of a real system:

- (i) It is a fact that low energy physics is only relevant to the part of the dispersion near the Fermi level. Therefore though the real dispersion near the Fermi level can dramatically deviate from the simple tight-binding band (sometimes even shows kink in the dispersion [24]), for practical purposes we still can model it by choosing an **effective scale** t that gives similar **Fermi velocity** v_F at the Fermi level (since $v_F = |d\varepsilon/d\mathbf{k}|_{\text{FS}} \propto t$). Thus in our context, Δ/t is equivalent to Δ/v_F , i.e. a greater Δ/t could mean a smaller v_F but does not necessarily mean a greater Δ . Obviously, we do not think “ t ” as the bandwidth of the real dispersion, which is not of our concern.
- (ii) On the **relative size** of Δ/v_F in LSCO and YBCO: Though there is a consensus that $\Delta_{\text{YBCO}} \sim 2\Delta_{\text{LSCO}}$, the v_F 's are very uncertain [25,24]. We therefore take v_F as a phenomenological input which is to be verified by future ARPES measurements, and v_F is thought as the dominant factor in the relative size of Δ/v_F .
- (iii) Note also that since v_F (or the effective t) is uncertain, we will compare all energies (e.g. ω , T , etc) only in terms of Δ .

The most important correction to the susceptibility should be the existence of Coulomb or AF correlations between the quasiparticles. Such correlations are believed to exist as a residual interaction between the renormalized particles, and they are conventionally treated by mean field decoupling as a nontrivial step beyond bare theories. Then the susceptibility is written into a RPA form as

$$\chi(\mathbf{q}, \omega) = \frac{\chi_o(\mathbf{k}, \omega)}{1 - V_{\mathbf{q}}\chi_o(\mathbf{k}, \omega)}, \quad (3)$$

where $V_{\mathbf{q}}$ can be the vertex of Hubbard repulsion U or AF interaction

$$J_{\mathbf{q}} = -\frac{|J|}{2}(\cos q_x + \cos q_y). \quad (4)$$

$J_{\mathbf{q}}$ is different from U essentially at being positive near \mathbf{Q}_{AF} and changing its sign to negative near $(0, 0)$. The RPA-type correction is important because it is perhaps the only way to treat correlation effect analytically.

III. EXCITATION AT BARE LEVEL — SURVEY OF BASIC PROPERTIES

We have given in this section a survey of the essential properties of the bare excitation spectrum. Their discussion will be given in Sec. IV.

A. Superconducting State

The SC state is described by $\Delta(T) \neq 0$, which results in a quasiparticle excitation gap and a SC coherence factor.

Figure 1 shows the frequency-evolution of the spectra for two typical cases of Δ/t . We have ignored the well-discussed quasielastic node-to-node IC peaks [26] at $(\pi + \delta_o, \pi \pm \delta_o)$ and $(\pi - \delta_o, \pi \pm \delta_o)$, and focused on the nesting IC peaks at $(\pi, \pi \pm \delta)$ and $(\pi \pm \delta, \pi)$. In general, as ω is increased, the intensity and widths of the peaks are increased, and spectrum at \mathbf{Q}_{AF} is filled in at some frequency near 2Δ which depends only on band geometry. When Δ/t is large, the fill-in is a stepwise jump of $\chi_o''(\mathbf{Q}_{AF}, \omega)$. This sharp increase of $\chi_o''(\mathbf{Q}_{AF}, \omega)$ has an important relation to the resonance at \mathbf{Q}_{AF} and will be further discussed in Sec. VI. The nesting IC peaks are seen to be sharpest at some intermediate frequencies before the filling in.

In contrast to the sharp, well-preserved and not-shifted peaks in the $\Delta/t \ll 1$ case [see Fig. 1(a)], the larger Δ/t calculation [see Fig. 1(b)] shows broader and biased peaks that clump into \mathbf{Q}_{AF} with increasing frequency. Such converging of the IC peak cluster was observed experimentally in YBCO and theoretically reproduced by us [12] and other groups [27,11,10]. Here we proceed to give its full explanation in Sec. IV. If the saddle vHS at $\mathbf{k} = (0, \pi)$ is far from the Fermi level, the IC structure will be destroyed after the peaks clump in at some $\omega/\Delta \lesssim 2$.

Some stray structures around the IC peaks always exist especially in the case of larger Δ/t and ω/Δ . When the RPA correction is introduced, they will become relatively weaker.

The main point here is that at $\omega \sim \Delta$, a system with moderate Δ/v_F (modeled by a moderate Δ/t) has its nesting peak broad and driven by ω to shift. We will discuss in Sec. IV that the shift direction actually depends on the orientation of the curvature of the FS near the gap nodes.

B. Normal State

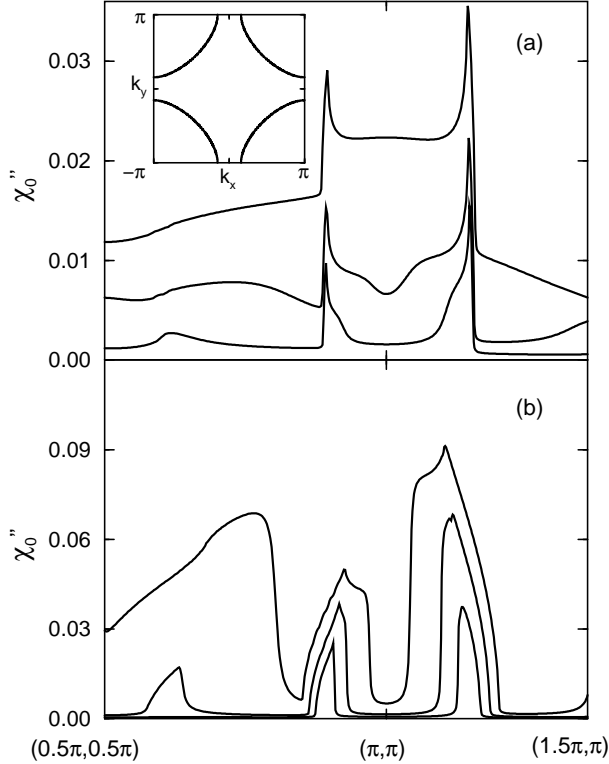


FIG. 1. Frequency evolution of the SC state $\chi''_o(\mathbf{q}, \omega)$ with different Δ/t is shown. (a) $\Delta/t = 0.03, \omega/\Delta = 1.0, 1.5,$ and 2.0 (from bottom to top); (b) $\Delta/t = 0.30, \omega/\Delta = 0.6, 1.0,$ and 1.4 (from bottom to top). In (b), the broad peak shifts at changing frequency, and some stray structure away from the IC peak is present. Including the RPA-correction [see Fig. 8(d)] will make the IC peaks and shifting effect more conspicuous. We particularly note that since we mean to describe two *different* systems in (a) and (b), the “ Δ ” or “ t ” in (a) and (b) are unrelated quantities. For both panels, $T = 0$, the dispersion is $t = 1, t' = -0.25,$ and $\mu = -0.65$. The FS is shown in the inset and the plots are along $\mathbf{q} = (0.5\pi, 0.5\pi) - (\pi, \pi) - (1.5\pi, \pi)$.

The normal state is described by $\Delta(T) = 0$, which leaves the bandwidth or the Fermi velocity as the only energy scale. Eq. (1) is then reduced to the Lindhard function

$$\chi_o(\mathbf{q}, \omega) = \sum_{\mathbf{k}} \frac{f(\xi_{\mathbf{k}}) - f(\xi_{\mathbf{k}+\mathbf{q}})}{\omega - \xi_{\mathbf{k}} + \xi_{\mathbf{k}+\mathbf{q}} + i\Gamma} \quad (5)$$

via $E_{\mathbf{k}} \rightarrow |\xi_{\mathbf{k}}|$, $|\xi_{\mathbf{k}}| = \xi_{\mathbf{k}}$ and $-\xi_{\mathbf{k}}$ when $\xi_{\mathbf{k}} > 0$ and $\xi_{\mathbf{k}} < 0$ respectively. The relation $f(-\xi_{\mathbf{k}}) = 1 - f(\xi_{\mathbf{k}})$ is also used.

Figure 2 shows some typical normal state spectra. The IC peaks are found to exist only at the regime $\omega/t \ll 1$. Such destruction of the normal state peaks by frequency qualitatively agrees with the experimental fact [28]. In that regime, increasing frequency broadens the peak and enhances the intensity, but do not shift the peaks. Similar to the discussion in previous subsection, $\omega/t \ll 1$ in our

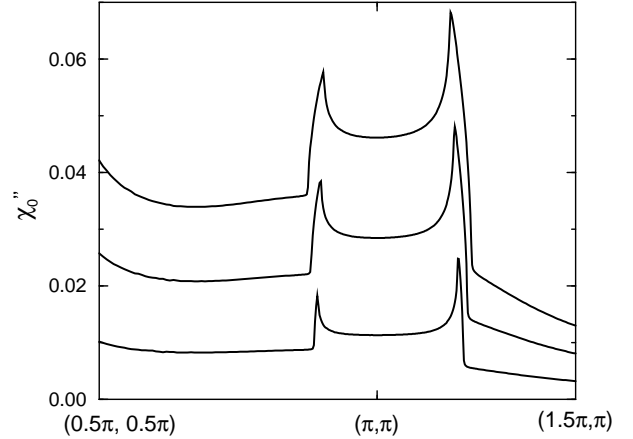


FIG. 2. Normal state (i.e. $\Delta = 0$) $\chi''_o(\mathbf{q}, \omega)$ at $\omega/t = 0.04, 0.10,$ and 0.16 (from bottom to top) is shown along $\mathbf{q} = (0.5\pi, 0.5\pi) - (\pi, \pi) - (1.5\pi, \pi)$. Such IC peaks exist only in the regime $\omega/t \ll 1$. Temperature $T = 0$ and the dispersion is $t = 1, t' = -0.25,$ and $\mu = -0.65$.

context could simply mean a steep dispersion at FS (i.e. large t) and does not necessarily mean a small ω .

C. Transition between Superconducting and Normal States

In the transition from SC to normal state, the gap is continuously diminished and hence the coherence factor. The restriction on transition in phase space is also relaxed. We will take an empirical relation $\Delta(T) = \Delta(0)[1 - (T/T_c)^4]^{1/2}$ [see inset in Fig. 3] at $T < T_c$ in our discussion.

If the IC peaks exist in the normal state, at entering the SC state [see Fig. 3(a)] it will be enhanced when $\omega/\Delta(0) > 1$ and suppressed if $\omega/\Delta(0) \sim 1$, and it will also be sharpened for $\omega/\Delta(0) < 2$ since spectral weight at \mathbf{Q}_{AF} will be gapped out.

Figure 3(b) shows a remarkable case of transition across T_c . For a system which was shown previously to have frequency-shifted IC peaks in the SC state [see Fig. 1(b)], increasing temperature broadens the peaks and shifts them towards \mathbf{Q}_{AF} . The peaks merge into a broad commensurate (or weakly IC structure) structure in the normal state. The change is drastic at $T \lesssim T_c$ where $\Delta(T)$ is rapidly changing.

The essential point here is the following. Given Δ of a system, when v_F (model by t) is such that Δ/v_F (modeled by Δ/t) is large enough to provide frequency-shifted IC peaks, the peaks will also be temperature-shifted and vanish in the normal state (since the condition $\omega/t \ll 1$ for the normal state peak to exist is necessarily violated at $\omega \sim \Delta$).

IV. EXCITATION AT BARE LEVEL

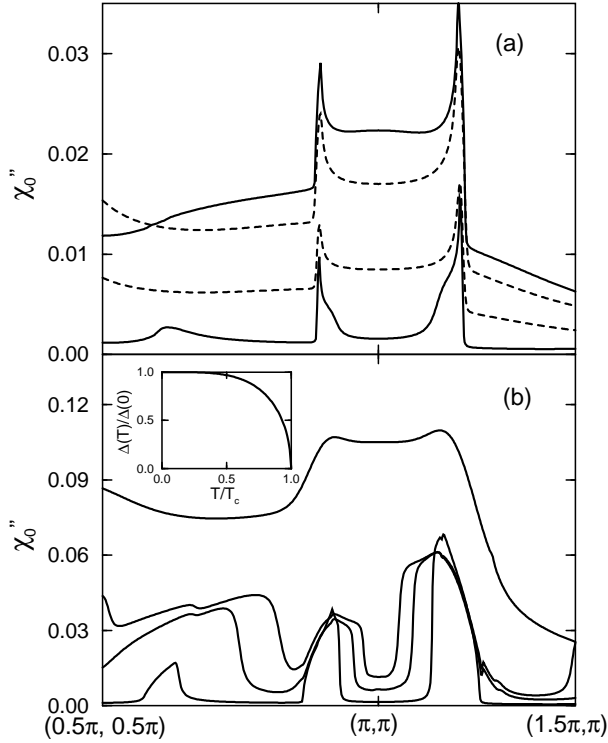


FIG. 3. Bare spectra $\chi''_o(\mathbf{q}, \omega)$ with different $\Delta(0)/t$ and $\omega/\Delta(0)$ at varying temperature. (a) $\Delta(0)/t = 0.03$: the solid lines show the $T = 0$ spectra at $\omega/\Delta(0) = 1.0$ and 2.0 (from bottom to top). The dashed lines have likewise frequencies but $T = T_c = 0.25\Delta(0)$. (b) $\Delta(0)/t = 0.30$ and $\omega/\Delta(0) = 1.0$: $T/T_c = 0, 0.80, 0.85$, and 1.0 (from bottom to top). $T_c = 0.25\Delta(0)$ and the assumed T -dependence of $\Delta(T)$ is shown in the inset. Heating converges the IC peak cluster in (b) to a commensurate structure. Note also that neither the “ Δ ” or “ t ” in (a) is related to that in (b). The dispersion used in both panels is $t = 1$, $t' = -0.25$, and $\mu = -0.65$. The plots are along $\mathbf{q} = (0.5\pi, 0.5\pi) - (\pi, \pi) - (1.5\pi, \pi)$.

— THE DYNAMIC LOCAL NESTING

The IC peaks are originated from the *umklapp* and inversion symmetry of the dispersion. This section discusses the properties of the bare excitation mentioned in Sec. III. Both the ω - and T -driven peak shifting effects are essentially due to the dynamic and local nature of the nesting effect.

We start to illustrate the mechanism by a zero temperature SC system where the bare spectrum is given by

$$\chi''_o(\mathbf{q}, \omega) = \frac{\pi}{4} \sum_{\mathbf{k}} \left[1 - \frac{\xi_{\mathbf{k}} \xi_{\mathbf{k}+\mathbf{q}} + \Delta_{\mathbf{k}} \Delta_{\mathbf{k}+\mathbf{q}}}{E_{\mathbf{k}} E_{\mathbf{k}+\mathbf{q}}} \right] \times [\delta(\omega - E_{\mathbf{k}} - E_{\mathbf{k}+\mathbf{q}}) - \delta(\omega + E_{\mathbf{k}} + E_{\mathbf{k}+\mathbf{q}})]. \quad (6)$$

The integrand consists of a coherence factor which reflects the non-time-reversal invariance nature of the magnetic measurement, and a δ -function that imposes the energy conservation rule.

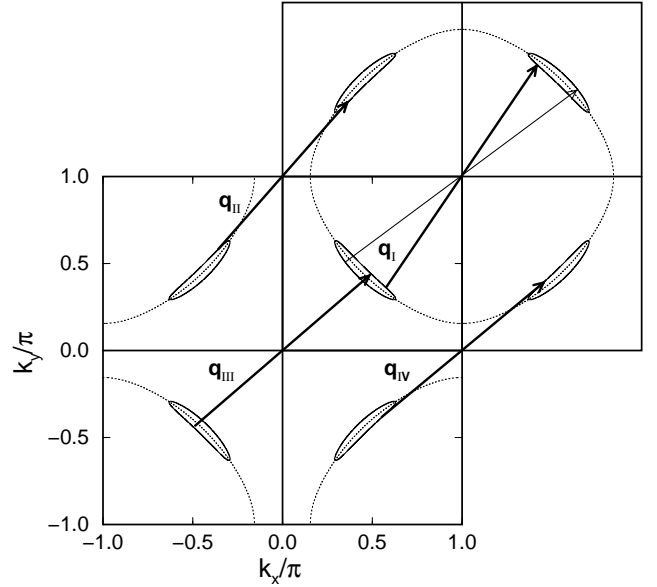


FIG. 4. Energy contour $E_{\mathbf{k}} = \omega/2$ in the extended BZ for $\omega = 1.0\Delta(0)$. Some arbitrary local-nesting vectors \mathbf{q}_I , \mathbf{q}_{II} , \mathbf{q}_{III} , and \mathbf{q}_{IV} are shown. The thick vector between above-FS contour piece have better nesting due to the smaller curvature. The FS is shown as dotted line, and the dispersion is $t = 1$, $t' = -0.25$, and $\mu = -0.65$. The gap here is chosen as $\Delta/t = 0.50$.

The role of the δ -function should be first discussed since it is the most dominant. It limits the contributing region of the phase space by the energy conservation $E_{\mathbf{k}} + E_{\mathbf{k}+\mathbf{q}} = \omega$. At $\omega \sim 0$, the only possibility is $E_{\mathbf{k}}$ and $E_{\mathbf{k}+\mathbf{q}}$ both ~ 0 . Therefore \mathbf{q} can only be vectors connecting the gap nodes, which are $\mathbf{Q}_{\delta_o} \equiv (\pi + \delta_o, \pi \pm \delta_o)$ and $(\pi - \delta_o, \pi \pm \delta_o)$, with $\delta_o = 2 \sin^{-1} \sqrt{[t - \sqrt{t^2 - t'\mu}] / [-2t']}$.

At $\omega > 0$, to satisfy $E_{\mathbf{k}} + E_{\mathbf{k}+\mathbf{q}} = \omega$, \mathbf{q} can be any momentum that connects points on the contours $E_{\mathbf{k}} = \omega_1$ and $E_{\mathbf{k}+\mathbf{q}} = \omega_2$, if $\omega_1 + \omega_2 = \omega$. These are strips of area stretched out from the gap node along the FS. For most \mathbf{q} , it only constitutes a featureless and “incoherent” background in the \mathbf{q} -space. To constitute a salient structure out of the background one needs to have extra factors that can stack extra weight onto the background. A situation that can further provide some weight is when $\omega_1 = \omega_2 = \omega/2$ and all the two frequency dependent contours become $E_{\mathbf{k}} = E_{\mathbf{k}+\mathbf{q}} = \omega/2$. It spans the whole FS when $\omega \rightarrow 2\Delta$. Now \mathbf{q} can “nest” two contours locally by passing through points $\mathbf{k}_o = (m\pi, n\pi)$ (where m and n are integers) in the BZ. It occurs because the ω -dependent contour is always locally parallel at $\mathbf{k}_o + \mathbf{k}$ and $\mathbf{k}_o - \mathbf{k}$ due to the dispersion $E_{\mathbf{k}}$ has the $\mathbf{k} \leftrightarrow -\mathbf{k}$ inversion and *umklapp* symmetry in the extended BZ. This nesting is thus *dynamic* and *local*.

As an example, we consider $\chi''_o(\mathbf{q}, \omega)$ at $\mathbf{q} \in [0 \sim 2\pi, 0 \sim 2\pi]$ and the integration over \mathbf{k} in evaluating χ''_o is

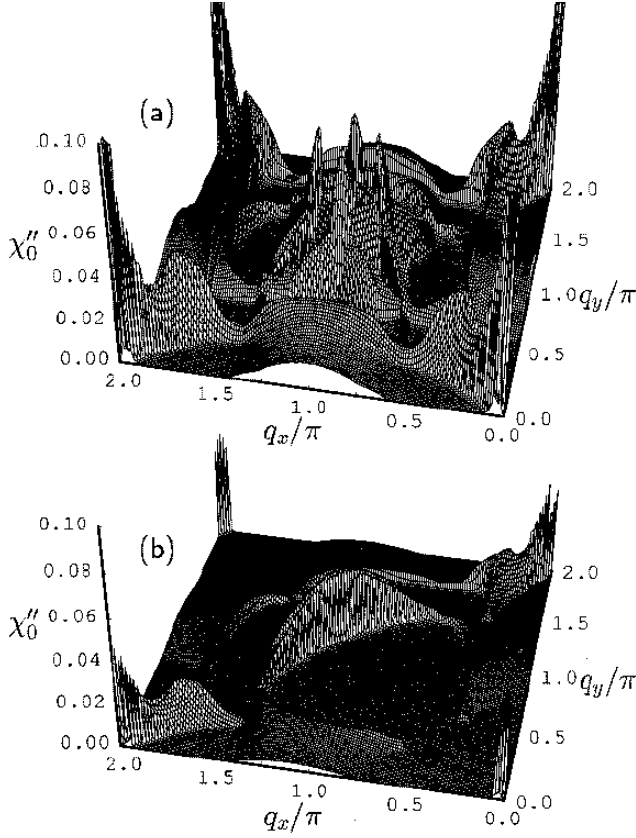


FIG. 5. (a) A bare spectrum $\chi''_0(\mathbf{q}, \omega)$ in the full \mathbf{q} -space at $\omega = 1.0\Delta(0)$. (b) a single branch of “ridge”, obtained when the integration over \mathbf{k} in Eq. (1) is done only over the quadrant $(k_x, k_y) \in [0 \sim \pi, 0 \sim \pi]$. Four of these 90-degree rotated branches superpose to give $\chi''_0(\mathbf{q}, \omega)$ in (a). Refer the dispersion parameters to Fig. 1(b).

run over $(k_x, k_y) \in [-\pi \sim \pi, -\pi \sim \pi]$. Fig. 4 illustrates the local-nesting at a frequency $\omega < 2\Delta$. In the integration over the first quadrant $(k_x, k_y) \in [0 \sim \pi, 0 \sim \pi]$, those local nesting vectors are shown as \mathbf{q}_I . Likewise, \mathbf{q}_{II} for the second, \mathbf{q}_{III} for the third, and \mathbf{q}_{IV} for the fourth quadrant.

Figure 5(a) shows the consequence of such local-nesting effect. The formation of the structure can be illustrated by an illuminating calculation, where the integration is done only over the first quadrant $(k_x, k_y) \in [0 \sim \pi, 0 \sim \pi]$. Then only one branch of the ridge-like structure is obtained [see Fig. 5(b)] and its orientation is the same as the contour in quadrant $(k_x, k_y) \in [\pi \sim 2\pi, \pi \sim 2\pi]$. The ends of the ridge are determined by $\Delta_{\mathbf{k}} = \omega/2$. The locus of the ridge in \mathbf{q} -space resembles the locus of the contour (which is approximately the FS) in \mathbf{k} -space but have twice the extension since the nesting vectors are twice the vectors describing the locus of the FS in \mathbf{k} -space [see Fig. 4].

An IC peak is a result of overlapping of two ridges at the symmetrical points $\mathbf{Q}_\delta = (\pi, \pi \pm \delta)$ and $(\pi \pm \delta, \pi)$, where $\delta = 2 \sin^{-1}[-\mu/(2t)]$, when $\omega > \omega_\delta \equiv$

$\Delta(T)[- \mu/(2t)]$. For those FS of open topology [see Fig. 4], the ridges overlap also at $\mathbf{Q}_{\delta'} = (\pi + \delta', \pi \pm \delta')$ and $(\pi - \delta', \pi \pm \delta')$ when $\omega > \omega_{\delta'} \equiv \Delta(T)\sqrt{\mu/t'}$, where $\delta' = 2 \sin^{-1} \sqrt{\mu/(4t')}$. The above expressions for δ_o, δ , and δ' are estimations since the ridges have finite thickness.

Frequency $\omega_{\delta'} \equiv \Delta(T)\sqrt{\mu/t'}$ is also the onset frequency of $\chi''_o(\mathbf{Q}_{AF}, \omega)$, since \mathbf{Q}_{AF} also connects equivalent points of $\mathbf{Q}_{\delta'}/2$ (also called the “hot spots”).

Due to the bending of the ridges [see Fig. 5], one will miss the nodal excitation point \mathbf{Q}_{δ_o} if one scan two nesting IC peaks at \mathbf{Q}_δ in their nearest distance direction. Therefore χ''_o will be seen as always gapped at any \mathbf{q} . Since this should be more prominent when Δ/t is small (which is likely the case of LSCO), this may explain the observation of a momentum independent spin gap by Lake *et al.* on LSCO [4].

A very peculiar feature which has been overlooked previously is the peak shifting behavior, brought by the difference of curvature of the contour pieces below and above the FS near the gap nodes. This occurs when the nodal FS segment has nonzero curvature and the contour $E_{\mathbf{k}} = \omega/2$ is appreciably opened up from it. In the geometry of FS shown in Fig. 4, the above-FS contour has a smaller curvature and can be nested more effectively. That causes the ridges to have biased cross-sections, which in turn causes the nesting peaks to have their apex biased to some direction [see Fig. 1(b)]. The opening up of the contour with ω increases the widths of the ridges and peaks, and therefore shifts the apex of the broad peaks [see Fig. 1(b)]. The broad and shifting behavior of the bare excitation peak are thus necessarily coexist.

Finite temperature in SC states drives the gap and thus changes the extensions of ridges both along and away from the FS. When T broadens the ridges away from FS, it simultaneously shifts the peaks apex like increasing ω . Besides, T always causes some smearing in all cases, the SC or the normal state.

When the dispersion at FS (i.e. v_F or t) is steep or the gap (Δ) is small, for $\omega \sim \Delta$, the contours are confined on the FS because its transverse extension in phase space $\delta\mathbf{k} \sim \Delta/|d\varepsilon/d\mathbf{k}|_{\text{FS}} = \Delta/v_F \ll \pi$ (this is equivalent to the condition $\Delta/t \ll 1$). The ridges and IC peaks formed are slim and no shift of peak is possible. For the peak to shift, a finite curvature of the FS is also necessary to provide the difference of curvature between the above- and below-FS contours.

The coherence factor has values between 0 and 2, and that can provide modification of the intensity as pointed out in the literature. The condition $\xi_{\mathbf{k}} \rightarrow 0$ at the FS tends to maximize the spin coherence factor to 2 at $\Delta_{\mathbf{k}}\Delta_{\mathbf{k}+\mathbf{q}} < 0$, and minimize it to 0 at $\Delta_{\mathbf{k}}\Delta_{\mathbf{k}+\mathbf{q}} > 0$. As our nesting vectors has $\Delta_{\mathbf{k}}\Delta_{\mathbf{k}+\mathbf{q}} > 0$, the ends of ridges are smoothly suppressed by the cutoff $\Delta_{\mathbf{k}} = \omega/2$. In the case of larger Δ/t , the condition $\xi_{\mathbf{k}} \rightarrow 0$ is not well satisfied at finite ω/Δ since the contour is opened up

appreciably from the FS. This weakens the suppression effect before cutoff, and the ridges will overlap at more sizable values and gives a higher contrast of the nesting IC peaks. It also lowers the threshold ω/Δ for the emergence of the peaks.

The normal state is the lift of the energy restriction by the gap, and the disappearance of coherence factor. The ridges now always span the whole \mathbf{q} -space and the nesting peaks always exist in principle. But due to replacing a stronger energy constraint (due to two-particle excitation) by a looser constraint (due to one-particle excitation), the transition now floods over regions far away from the FS and makes the widths of ridges dispersed and the nesting peaks less distinguishable. Especially now the transition near \mathbf{Q}_{AF} is filled high for hole-like FS.

Albeit the underlying cause of formation of the ridges and nesting peaks (*umklapp* and \mathbf{k} -inversion symmetry) is irrelevant to the existence or not of the SC gap, there are still some upper limits on ω/Δ or ω/t for the IC peaks to exist. Since increasing ω/t broadens the ridges, the ridge and peak structure will be always destroyed at very high ω/t . The same is true for very high T/t where the excitation is deconfined from the FS. It is easier for the peak to survive in the SC state because the near \mathbf{Q}_{AF} transition is kept away at $\omega/\Delta < 2$ [see Fig. 3(b)].

To summarize, at low ω/t and T/t , the nesting IC peaks should always exist in bands with *umklapp* and inversion ($\mathbf{k} \leftrightarrow -\mathbf{k}$) symmetry. In the SC state, it can be driven by ω or T to shift when Δ/t is appreciable and the nodal FS is curved.

V. RPA-CORRECTED EXCITATION

In this section we will discuss the effect of RPA correction on the frequency-driven shifting effect of the IC peaks. We start with a brief discussion of the essential features of the RPA spectrum.

The RPA spectrum is given by

$$\chi''(\mathbf{q}, \omega) = \frac{\chi_o''(\mathbf{q}, \omega)}{[1 - V_{\mathbf{q}}\chi_o'(\mathbf{q}, \omega)]^2 + [V_{\mathbf{q}}\chi_o''(\mathbf{q}, \omega)]^2}. \quad (7)$$

It can be viewed as a scaling of χ_o'' by the Stoner factor $[(1 - V_{\mathbf{q}}\chi_o')^2 + (V_{\mathbf{q}}\chi_o'')^2]$, which is greater or equal to zero.

Figure 6 shows that Stoner factor $s = [(1 - V\chi_o')^2 + (V\chi_o'')^2]$ versus $V\chi_o'$ for various χ_o''/χ_o' . It summarizes all features of the RPA correction in a lucid way. For instance, at the regime of small χ_o''/χ_o' , RPA spectra with $V < 1/\chi_o'$ is just a scaling (i.e. $s \neq 0$, could be magnification or suppression) of the bare spectra; while RPA spectra with $V \simeq 1/\chi_o'$ are resonances (i.e. $s \sim 0$) with damping χ_o'' . For large χ_o''/χ_o' , s is greater than 1 in most regions, which means that for most choices of V the RPA correction has only suppression effect. This can happen in systems with large χ_o'' due to band singularity.

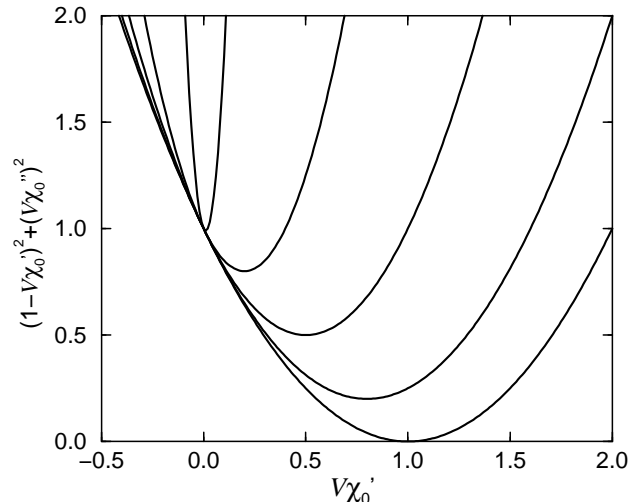


FIG. 6. The Stoner factor $[(1 - V\chi_o')^2 + (V\chi_o'')^2]$ is plotted against $V\chi_o'$ for $\chi_o''/\chi_o' = 0, 0.5, 1.0, 2.0,$ and 10 (from bottom to top).

In reality, the RPA resonance could be unlikely to occur in systems with well-behaved properties near the Fermi level by the following reason. For any stable system, $V_{\mathbf{q}}$ should be sufficiently away from the instability boundary $V_{\mathbf{q}} = 1/\chi_o'(\mathbf{q}, \omega = 0)$ [see Fig. 7 for an example]. When there is no singular sources such as the van Hove singularity near the Fermi level, $\chi_o''(\mathbf{q}, \omega)$ changes smoothly with ω and $\chi_o'(\mathbf{q}, \omega)$ is inert to change of ω (due to the Kramers-Kronig relation). Theoretically a fine tuning of the interaction strength is then required to get a resonance. In such systems, absence of instability at zero ω is likely to imply absence of resonance at nonzero ω .

Figure 8 illustrates the effect of RPA correction on the peak shifting behavior. We have considered antiferromagnetic interactions $J_{\mathbf{q}}$ which do not cause resonance (weak coupling). In the case of moderate Δ/t , sharp local minima of $1/\chi_o'$ [Fig. 8(c)] appear at the sharp edges of the bare IC peaks due to the Kramers-Kronig relation. This is nontrivial as it results in more spectacular shifting of the IC peaks [compare Fig. 8(d) and Fig. 1(b)]. On the other hand, in the case of small Δ/v_F , the fixed incommensuration behavior is maintained [Fig. 8(b)] due to the “quiescent” $1/\chi_o'$ [Fig. 8(a)]. We conclude that the weak coupling RPA correction do not alter the original behaviors of the IC peaks, and the LSCO data can be described by small Δ/v_F and weak coupling RPA correction.

VI. EXCITATION SPECTRUM AND \bar{M} -POINT VAN HOVE SINGULARITY

This is a RPA spin excitation theory for the recently reported INS data on YBCO. For simplicity, we have

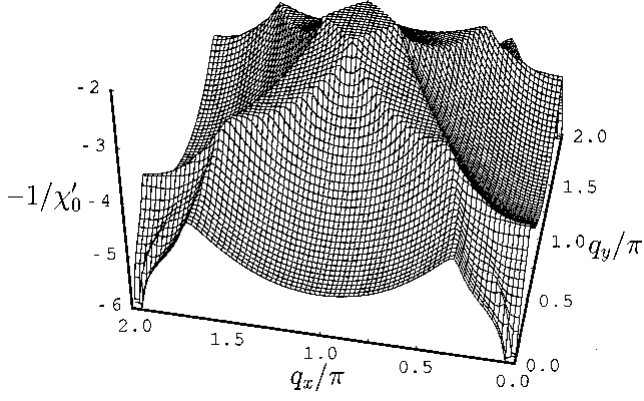


FIG. 7. A typical SC state $-1/\chi'_o(\mathbf{q}, \omega = 0)$ in \mathbf{q} -space. The no-instability bound of the interaction strength is $V_{\mathbf{q}} < 1/\chi'_o(\mathbf{q}, \omega = 0)$. For $V_{\mathbf{q}} = J_{\mathbf{q}}$, $|J| < 1/\chi'_o(\mathbf{q} \sim \mathbf{Q}_{AF}, \omega = 0) \simeq 2.2t$ in this case. The plot has $T = 0$, $\Delta/t = 0.03$, and band dispersion $t = 1$, $t' = -0.25$, and $\mu = -0.65$.

mimic the realistic *extended*-saddle-vHS at the proximity of Fermi level [19,22] by simple saddle-vHS just beneath Fermi level. It is believed that in RPA theories they will be qualitatively the same. Nevertheless its extended nature is crucial for bare theory to have quantitative agreement with experiments [27].

A number of comprehensive theories including both commensurate and IC excitation [10,11,27,12–14] were explored since the discovery of the behavior in YBCO. It is important to note that all of them are Fermi-liquid-like theories, and most are RPA theories [10,11,13,14]. The possibility of a bare theory was investigated by Abrikosov [27,29] and us [12]. The commensurate peaks in bare theories are generally weaker, broader, and occurs at $\omega_o \gtrsim 2\Delta$. That is in contrast to the much stronger and sharper one in χ'' that occurs at $\omega_o < 2\Delta$. However, recently it has been shown that incorporating the extended-vHS [27] into bare theory can also give peak intensity and width in reasonable agreement with experiments. Attempting to rely on the criterion ω_o being less or greater than 2Δ for choosing a theory also encounters the subtleties in the determination of the SC gap. Especially in the underdoped samples where there are still controversies on whether the SC gap and the pseudogap are the same gap [30–32]. Therefore either $\omega_o \gtrsim 2\Delta$ (see discussion in Ref. [29]) or $\omega_o < 2\Delta$ (e.g. in the underdoped compounds) can be occasionally favored. As a result we believe that at present there is no clear evidence here to favor either scenarios. Recently the IC peaks have received more attention because of their frequency-shifted behavior. Most of the present scenarios for it are based on the nesting effect which depends mainly on the nodal FS, except one recently proposed by Abrikosov [27] depends on the band mass at the extended-vHS region. The discussion of the temperature-shifted IC peaks has been missing from the literature.

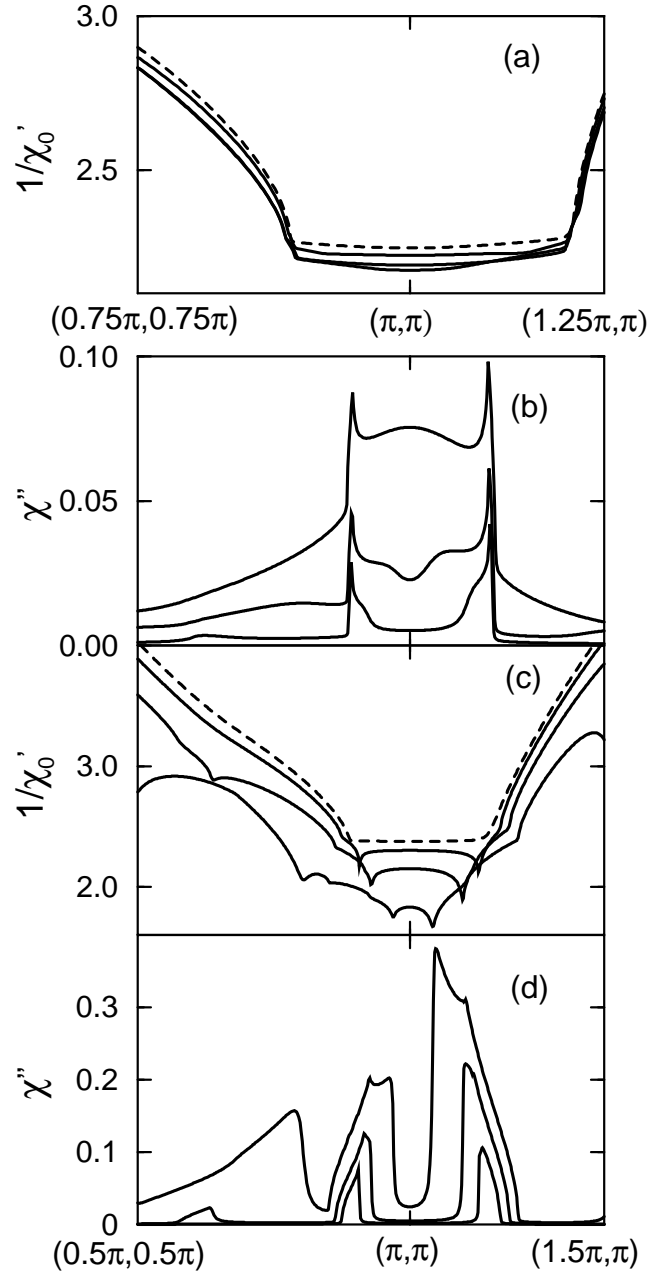


FIG. 8. RPA effect (with no resonance) on two systems with small and moderate Δ/t . All graphs except (a) are plotted along $\mathbf{q} = (0.5\pi, 0.5\pi) - (\pi, \pi) - (1.5\pi, \pi)$. For the case of $\Delta/t = 0.03$ and $|J|/t = 1.0$: (a) $1/\chi'_o(\mathbf{q}, \omega)$ is shown [along $\mathbf{q} = (0.75\pi, 0.75\pi) - (\pi, \pi) - (1.25\pi, \pi)$] at $\omega/\Delta = 0$ (dashed line), 1.0, 2.0 and 1.5 (solid lines at \mathbf{Q}_{AF} from top to bottom); Correspondingly, (b) $\chi''(\mathbf{q}, \omega)$ is shown at $\omega/\Delta = 1.0, 1.5$ and 2.0 (from bottom to top). For the case of $\Delta/t = 0.30$ and $|J|/t = 1.0$: (c) $1/\chi'_o(\mathbf{q}, \omega)$ is shown at $\omega/\Delta = 0$ (dashed line), 0.60, 1.0 and 1.4 (solid lines from top to bottom); Correspondingly, (d) $\chi''(\mathbf{q}, \omega)$ is shown at $\omega/\Delta = 0.6, 1.0$ and 1.4 (from bottom to top). Note the sharp minima of $1/\chi'_o$ in (c) and its discussion in the text. Temperature $T = 0$ and the corresponding bare spectra were shown previously in Fig. 1.

With a sufficiently strong correction strength, it is always possible to have a RPA resonance at \mathbf{Q}_{AF} . The reason is since any susceptibility function or interaction vertex on the lattice is symmetric at $\mathbf{Q}_{AF} + \delta\mathbf{q} \rightarrow \mathbf{Q}_{AF} - \delta\mathbf{q}$, they always have an extremum at \mathbf{Q}_{AF} [e.g. see Fig. 7] and thus one can always have $1 - V\chi'_o = 0$ locally at \mathbf{Q}_{AF} .

The dispersion taken here to mimic the YBCO dispersion has a hole-like FS and a simple saddle-vHS at $\overline{M} = (0, \pi)$ slightly beneath the Fermi level ($\xi_{\mathbf{k}=\overline{M}}/\Delta = -0.5$). The interaction is chosen as an antiferromagnetic $J_{\mathbf{q}}$ with $|J|/t = 1.6$. At $T = 0$, a commensurate resonance occurs at $\omega/\Delta = 1.5$. The momentum dependence of the RPA spectrum and $1/\chi'_o$ are shown in Fig. 9, at different frequencies and zero temperature. The onset of $\chi''(\mathbf{Q}_{AF}, \omega)$ and the minimum of $1/\chi'_o(\mathbf{Q}_{AF}, \omega)$ occurs at $\omega/\Delta = 1.77$.

A new feature appears at $\omega > \omega_o(T = 0)$ due to the shallow saddle-vHS. The discommensuration is seen to increase at increasing frequency [see Fig. 9(d)]. It is also due to a dynamic local nesting effect similar to that at $\omega \rightarrow \omega_o$ from below. Owing to the shallow flat band at \overline{M} , the nesting contours $E_{\mathbf{k}} = \omega/2$ at high frequencies necessarily have smaller curvature at those segments below FS, and can be more effectively nested locally [see Fig. 10]. The peak profile here is weak because the below- and above-FS contours are too far apart to coherently form a ridge. The RPA correction has an effect similar to that at $\omega < \omega_o(T = 0)$.

Replacing the saddle-vHS by an extended-saddle-vHS do not affect the IC excitation at $\omega < \omega_o$ since only the nodal FS is of concern. Neither the diverging discommensuration at $\omega > \omega_o$ will be affected since the switch-over of the smaller and larger curvature energy contours should also occur.

The large change in $1/\chi'_o$ at $\omega/\Delta = 0 \sim 2$ is a result of the large jump at the onset of $\chi''_o(\mathbf{Q}_{AF}, \omega)$ (at $\omega_{\delta}/\Delta(T) = \sqrt{\mu/t'} \simeq 1.8$). The onset is sharp and large due to the enhancement by the spin coherence factor (at $\Delta_{\mathbf{k}}\Delta_{\mathbf{k}+\mathbf{Q}_{AF}} < 0$), and the picking up of states around the shallow vHS at \overline{M} (at a depth of $\xi_{\mathbf{k}=\overline{M}} = 4t' - \mu$) by the δ -function [see Eq. (6)]. This widens the window and lowers the threshold for the interaction strength giving resonance. This may partially account for the existence of the commensurate peak in YBCO and BSCCO, but not in LSCO. The RPA effect at \mathbf{Q}_{AF} is effectively turned off when ω is increased beyond the maximum of $\chi''_o(\mathbf{Q}_{AF}, \omega)$, since $1/\chi'_o(\mathbf{Q}_{AF}, \omega)$ recedes rapidly from zero then [see Fig. 9(c)]. Since the onset frequency scales with $\Delta(T)$, the RPA commensurate resonance is necessarily softened by temperature. But the softening could be very little. The reason is that as $\Delta(T)$ gets smaller, divergence in $\chi'_o(\mathbf{Q}_{AF}, \omega)$ gets smaller and will fail to fulfill the resonance condition $\chi'_o(\mathbf{Q}_{AF}, \omega) = 1/V(\mathbf{Q}_{AF})$ for a given $V(\mathbf{Q}_{AF})$. The peak could cease to exist before its softening is really detected. The case for the softening of the commensurate peak in a bare theory is similar [12].

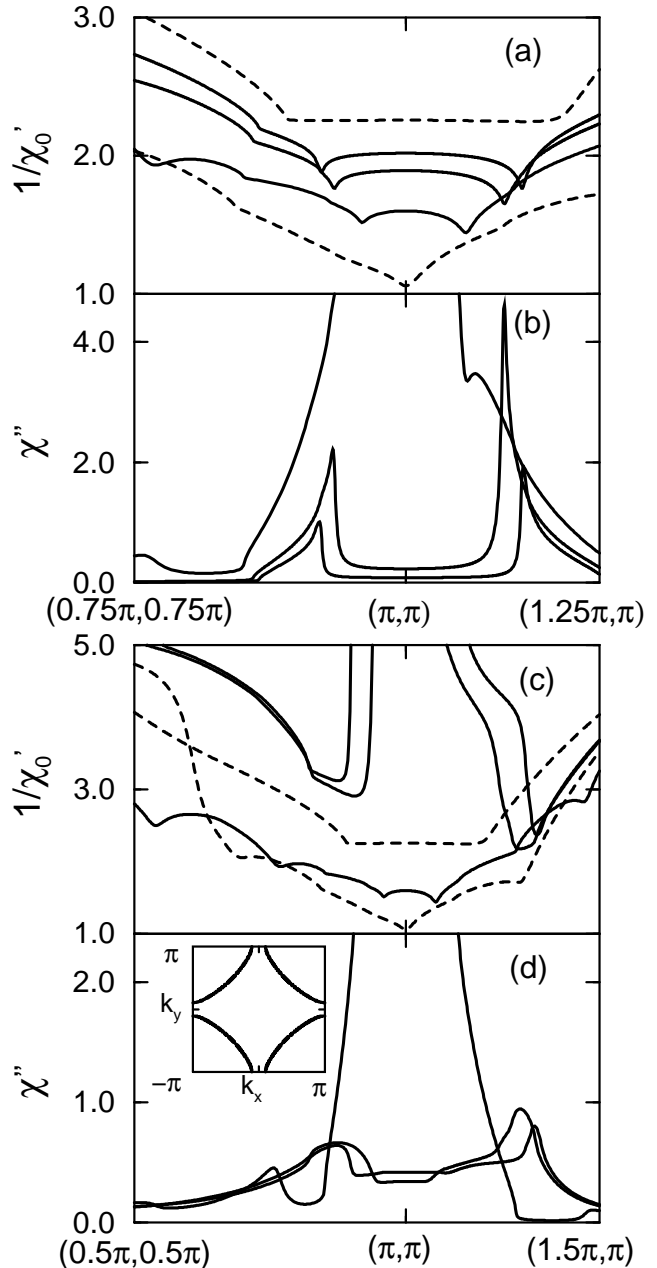


FIG. 9. Frequency-driven peak shifting at different frequency regimes : (a) $1/\chi'_o(\mathbf{q}, \omega)$ at $\omega/\Delta = 1.0, 1.2$, and 1.5 [solid lines from top to bottom]; (b) $\chi''(\mathbf{q}, \omega)$ at $\omega/\Delta = 1.0, 1.2$, and 1.5 [at decreasing incommensurability along $(\pi, \pi) - (1.25\pi, \pi)$]. (c) $1/\chi'_o(\mathbf{q}, \omega)$ at $\omega/\Delta = 1.5, 2.3$, and 2.5 [solid lines at increasing “incommensurability” of the minima along $(\pi, \pi) - (1.5\pi, \pi)$]; (d) $\chi''(\mathbf{q}, \omega)$ at $\omega/\Delta = 1.5, 2.3$, and 2.5 [at increasing incommensurability along $(\pi, \pi) - (1.5\pi, \pi)$]. The dashed lines from top to bottom in (a) and (c) show $1/\chi'_o$ at $\omega/\Delta = 0$ and 1.77 respectively. χ'' in (b) and (d) are calculated with $|J|/t = 1.6$, and the commensurate resonance occurs at $\omega = \omega_o(T = 0) = 1.5\Delta(0)$. We have truncated the strong commensurate peak for obvious reason. $T = 0$, the quasiparticle dispersion is $t = 1$, $t' = -0.20$, $\mu = -0.65$, and $\Delta = 0.30$ (gives $\xi_{\mathbf{k}=\overline{M}}/\Delta = -0.5$). The inset shows the FS. The broadening taken for all the calculations in this section is $\Gamma/t = 0.008$.

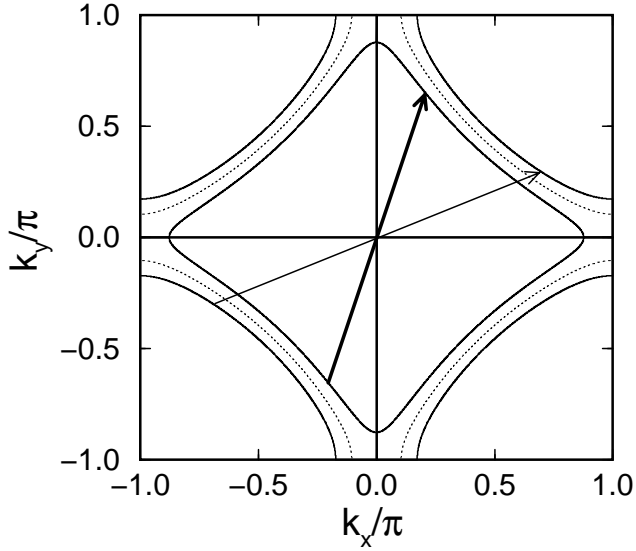


FIG. 10. Energy contour $E_{\mathbf{k}} = \omega/2$ for $\omega = 2.5\Delta(0) > \omega_o(T = 0)$. The thick local-nesting vector between *below*-FS contour has more pronounced nesting effect (compared to the thin vector) due to the smaller curvature. We remind that the dispersion here has a saddle-vHS near to Fermi level (refer the exact parameters to Fig. 9). The FS is indicated as dotted line.

Figure 11 plots the temperature-evolution of a low frequency spectrum in momentum space. The most notable should be the softened commensurate resonance at $\omega \lesssim \omega_o(T = 0)$. When the system is cooled down from above T_c , the broad and weak commensurate peak in the normal state grows into a sharp and strong peak at some temperature just below T_c , then it is split up into IC peaks and recede from \mathbf{Q}_{AF} , to a fixed location at low temperature. The weak IC structure at $\omega > \omega_o(T = 0)$ in SC state is found to be simply smeared off to a broad commensurate at warming up to the normal state [33].

Note that the observed relative excitation intensity in the course of the evolution [see Fig.4 in Ref. [3]] can only be obtained correctly in $\chi''(\mathbf{q}, \omega)$ via an appreciable interaction strength. Though the “shoot and split” behavior of the $\omega < \omega_o(T = 0)$ spectrum at cooling down is already contained in a bare theory invoking vHS effect for the commensurate peak [12], the normal state commensurate structure always incorrectly has an intensity higher than the low temperature IC structure in $\chi''(\mathbf{q}, \omega)$ [see, for example, a similar case in Fig. 3(b)].

A weak and broad commensurate structure is always seen in the normal state at all frequencies [see Fig. 12] as what is observed in experiments [3,2]. It is due to the enhancement by the saddle-vHS and RPA correction. For the model system considered here, its intensity reaches a maximum at some $\omega/\Delta(0) \simeq 0.4$ as a result of the competition between χ''_o and RPA enhancement.

In summary, the diverging incommensurability at $\omega > \omega_o$ in the SC state is accounted by the approaching of

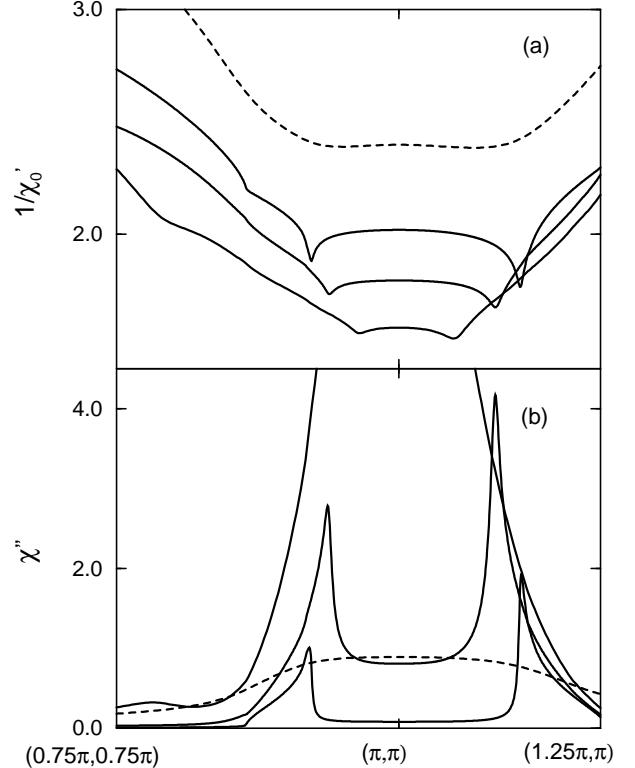


FIG. 11. Temperature-driven peak shifting at low frequency regime : At $\omega = 1.0\Delta(0) < \omega_o(T = 0)$, (a) $1/\chi'_o(\mathbf{q}, \omega)$ is shown at $T/T_c = 0, 0.8, 0.88$ (solid lines from top to bottom), and 1.0 (dashed line); (b) $\chi''(\mathbf{q}, \omega)$ is shown at $T/T_c = 0, 0.8, 0.88$ (solid lines at decreasing incommensurability), and 1.0 (dashed line). The weak commensurate structure in the normal state is seen to grow into a strong peak at $T = 0.88T_c \lesssim T_c$, then splits into IC peaks which recede from \mathbf{Q}_{AF} at $T \rightarrow 0$. The strong commensurate peak is truncated for obvious reason. $T_c = 0.25\Delta(0)$, and the T -dependence of $\Delta(T)$ is assumed as the same as in Fig. 3(b). Other parameters are referred to Fig. 9.

\overline{M} -point vHS to the Fermi level; the normal state broad commensurate structure at any frequency also finds a natural explanation in it. The recent observation on the relative excitation intensity in the normal and SC state prefers a RPA theory in the resonance regime more than the bare theories, though the gross features of the bare and RPA spectra are the similar. Including an underdoped sample (by Arai *et al.* [2]) and a nearly optimally doped sample (by Bourges *et al.* [3]), the converging and diverging shifting of the IC peaks has a transparent explanation in the FL picture.

VII. ANISOTROPY EFFECT

Anisotropy effect in the high- T_c cuprates was discussed before by Rendell and Carbotte [34]. The effect is believed to be important in systems such as the orthorhombic

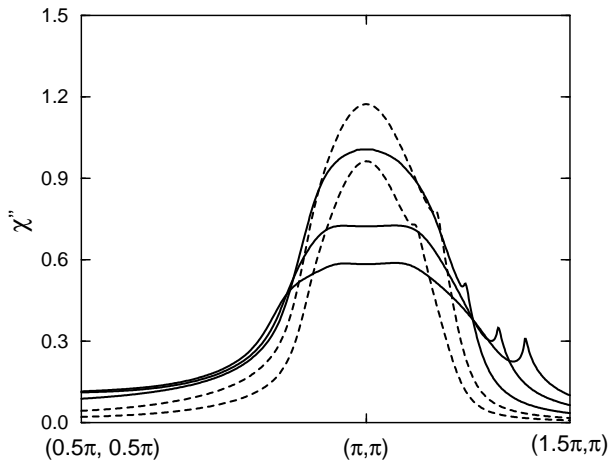


FIG. 12. The broad commensurate peak of normal state $\chi''(\mathbf{q}, \omega)$ at $\omega/\Delta(0) = 0.2, 0.4$ (dashed lines from bottom to top), 0.8, 1.4, and 2.0 (solid lines from top to bottom). $T = T_c = 0.25\Delta(0)$. Refer those not stated parameters to Fig. 9.

bic crystals or the chained-YBCO. In those systems, anisotropy may either exist in the band dispersion or enter into the SC order parameter, or exist in both. It was pointed out in Ref. [34] that if only one of those two kinds of anisotropy exist in the system, it can be distinguished by the criterion that the gap anisotropy exist only in the SC state while the dispersion anisotropy persists into the normal state. Some important effects of it which can be seen in INS spectrum are, if there is an admixture of s -component in the d -wave gap then there should be a rendering of the four-fold symmetry of the quasielastic node-to-node IC peaks to two-fold, and regardless of the anisotropy source a difference of the nesting IC peak intensities on different crystal axis should be observed.

We will discuss here a case of anisotropy in the gap, the existence of an s -component and the SC order parameter has the form $\Delta_{\mathbf{k}} = \Delta(T)[as_{\mathbf{k}} + (1-a)d_{\mathbf{k}}]$, where $s_{\mathbf{k}} = 1$ and $d_{\mathbf{k}} = (\cos k_x - \cos k_y)/2$. The existence of an s -component is suggested by the tunneling experiments [35–37] and its percentage is at $a \sim 0.2$. It was discussed in Ref. [34] at low frequencies, but in order to clearly distinguish the effect we think that it is necessary to study its ω -dependence.

Figure 13 shows the contrast of the nesting IC peaks along different crystal axis at different ω , on a system with reasonable size of s -component in the gap. The difference in peak intensities is seen to be most prominent at low ω , and rapidly decreased at increasing frequency. Since the data by Mook *et al.* (on a detwinned orthorhombic $\text{YBa}_2\text{Cu}_3\text{O}_{6.6}$) [23] is at a somewhat low frequency 24 meV $\sim \Delta(0)$, we believe data on a wider ω range is desirable in order to make definite statement on the origin of the one-dimensional nature.

The difference in peak intensities can be easily explained by the picture given in Sec. IV. The twofold sym-

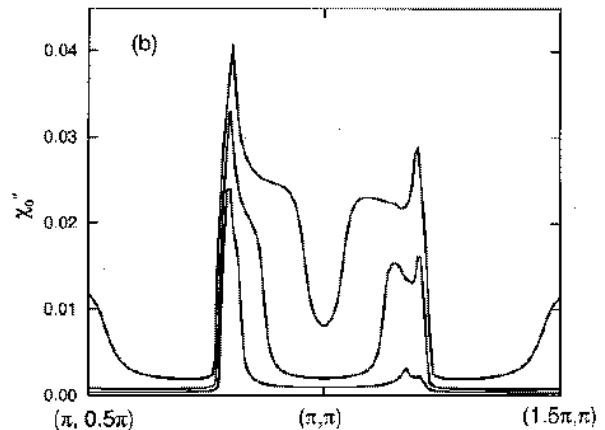
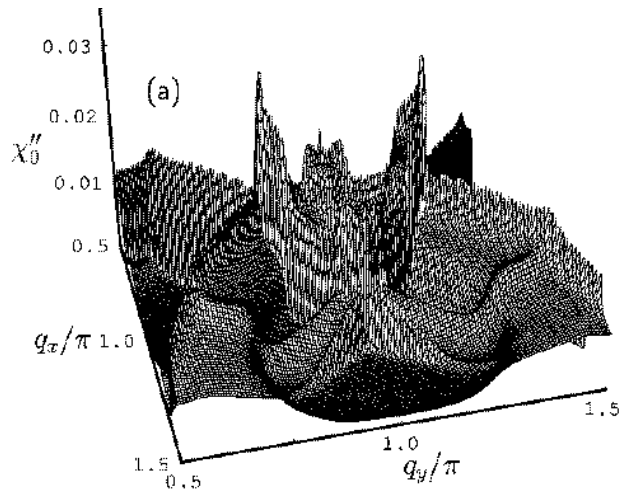


FIG. 13. Anisotropic SC state $\chi''_0(\mathbf{q}, \omega)$ (a) in the full \mathbf{q} -space at $\omega/\Delta = 1.0$, and (b) along $\mathbf{q} = (\pi, 0.5\pi) - (\pi, \pi) - (1.5\pi, \pi)$ at $\omega/\Delta = 0.6, 0.9$, and 1.2 (from bottom to top). The difference in height of the peaks on different axis is more spectacular at low frequencies. The SC order parameter is taken as $\Delta_{\mathbf{k}} = \Delta[0.2s_{\mathbf{k}} + 0.8d_{\mathbf{k}}]$, where $\Delta = 0.10$, $s_{\mathbf{k}} = 1$, and $d_{\mathbf{k}} = (\cos k_x - \cos k_y)/2$. $T = 0$ and the dispersion is $t = 1$, $t' = -0.25$, and $\mu = -0.65$.

metric spectrum has the node-to-node excitation closer to one of the two crystal axis, and excitation away from the nodal excitation is suppressed by the coherence factor, therefore the peaks on one of the axis has lower intensity. This can only dominate at frequencies as low as $\sim \Delta$ and excitation along the FS has not been fully opened up.

We have presented here an anisotropy effect suggested by the tunneling experiment and it can introduce one-dimensional feature into the INS spectrum (other possibility is also suggested in Ref. [9]). The frequency dependence of the contrast of IC peak intensity should act as a criterion to compare with the Stripe interpretation which has no frequency dependence. Furthermore such gap anisotropy effect should vanish in the normal state.

VIII. DISCUSSION AND CONCLUSIONS

We have presented a thorough study on the basic properties of the spin susceptibility and have summarized our findings and comparisons with experiments at the end of each section.

Some possible departure of our conclusions from reality should be mentioned. The presence of impurity in real systems destroys the exact translational symmetry and mixes states of different momentum, which are also the energy eigenstates. Such process necessarily relaxes the energy conservation selection of the transition region in phase space. The effect should be significant in low energy processes in the SC state where there is inhomogeneous gapping out of phase space by the d -wave gap. For example, it may pull down the lower threshold for the existence of the nesting IC peaks [38]. We have also taken a simple d -wave in the discussion which is just meant to describe a symmetry with four nodes and change of sign. The actual \mathbf{k} -dependence of the gap should exhibit some deviation from pure d -wave since other factors such as interlayer tunneling [39] or correlation effects *etc.* may influence. The important case of possessing a s -component was discussed in Sec. VII. The realistic dispersion at the FS also shows deviation from our simple tight-binding band, the most well known of all should be the presence of extended-vHS. Therefore all numerals we give are qualitative.

To a qualitative level, the “inconsistency” between INS spectra of LSCO and YBCO as mentioned in Sec. I can find a consistent picture in the FL interpretation. They could be systems in different regimes of the ratio Δ/v_F . The observations on LSCO [as discussed in Sec. III and Sec. V]: the wide existing IC excitation with incommensurability depends only on doping, can be ascribed to a small Δ/v_F of the system. The observations on YBCO [as discussed in Sec. III and Sec. VI]: including the ω - and T -driven shifted IC peaks in SC state, and normal state broad commensurate peak, can be all ascribed to an appreciable Δ/v_F of the system. The diverging incommensurability at $\omega \geq \omega_o$ in SC state are ascribed to the approaching of the \bar{M} -point vHS to the Fermi level. Though bare and RPA theories could be qualitatively similar, RPA theories can describe the temperature evolution of the excitation intensity more adequately. A peculiar but straightforward conclusion for the commensurate resonance is it can occur at $\omega \lesssim \omega_o(T = 0)$ when $T \lesssim T_c$, either in the bare [12] or RPA theories. This naturally explains the observed enhancement of scattering intensity at \mathbf{Q}_{AF} in that regime [see Fig.4(c) in Ref. [3]].

We would like to point out that while the observed commensurate peak in the SC state could easily find an interpretation as a resonance, as it occurs at a small frequency window; the lower intensity broad commensurate peak in the normal state which is observed at *any* frequency is hard to be interpreted in terms of a resonance. In our scenario this is a natural consequence of the over-

lap of broad IC peaks, with further enhancement by the \bar{M} -point vHS and RPA-correction.

On the ratio Δ/v_F of LSCO and YBCO, there should be a consensus that the SC gap of LSCO (~ 10 meV) is a fraction of that of YBCO (~ 30 meV). Due to the low resolution in the determination of electronic dispersion (the resolution in ARPES measurements is about 10-40 meV), presently v_F in most material could not be precisely determined [40,25,24] and neither the ratio Δ/v_F . Therefore in this paper we have meant only a first-step qualitative study, and did not predict any precise figure for v_F of different systems. But it is still important to note that in our scenario, v_F of YBCO should be at least several times smaller than that of LSCO .

In the literature, there are also other approaches [10,11,27,41] to the issue. As we do, Ref. [10] also simultaneously accounts for both the LSCO and YBCO data, but does not elaborate on how the difference in the behavior of the IC peak arises. Furthermore, it is predicted that a commensurate peak should also exist in LSCO. Ref. [11] addresses only the YBCO data by using a refined tight-binding band. It is also not shown explicitly that how the IC peaks are shifted. Moreover, the relation to the LSCO data is not mentioned. Ref. [27] obtains the commensurate and shifting IC peaks from the quasiparticle masses at the extended-saddle-vHS region, while the data of LSCO is also not mentioned. In our present work, we assume that the IC peaks in LSCO and YBCO have the same origin, and have related the different behaviors of them to their individual Fermi velocities v_F . An explicit explanation of the shifting behavior is also given. The approach in Ref. [41] is very different from ours as it interprets the shifting of the IC peak as the downward dispersion of a spin wave mode. Our approach can also easily address the shifting of IC peak caused by temperature change, which is so far only discussed by us.

There are some bewildering stems from our work. In the underdoped cuprates, anomalies such as the pseudo-gap phenomenon or the destruction of FS [42] are seen near the maximum gap region and it is likely that the FL picture is to breakdown at that region. But now the FL behavior near the maximum gap region is an important ingredient in our scenario on the YBCO, and our coverage includes both the underdoped and optimally doped YBCO. It seems that to some extent the FL behavior is still retained in the response to INS measurements.

In conclusion, albeit the FL picture on the cuprates is recently questioned by many experiments, most behaviors of the recent INS data are still well described in terms of the traditional Fermi liquid picture.

ACKNOWLEDGMENTS

KKV acknowledges the scholarship from NSC of Taiwan under grant No.89-2112-M-003-009. We thank P. Bourges *et al.* for sending us their results prior to publi-

cation. We also want to thank A. Abrikosov for sending us his preprint as well as useful correspondences.

-
- [1] K. Yamada, C.H. Lee, K. Kurahashi, J. Wada, S. Wakimoto, S. Ueki, H. Kimura, Y. Endoh, S. Hosoya, G. Shirane, R.J. Birgeneau, M. Greven, M.A. Kastner, and Y.J. Kim, *Phys. Rev. B* **57**, 6165 (1998).
- [2] M. Arai, T. Nishijima, Y. Endoh, T. Egami, S. Tajima, K. Tomimoto, Y. Shiohara, M. Takahashi, A. Garrett, and S.M. Bennington, *Phys. Rev. Lett.* **83**, 608 (1999).
- [3] P. Bourges, Y. Sidis, H.F. Fong, L.P. Regnault, J. Bossy, A. Ivanov, and B. Keimer, *Science* **288**, 1234 (2000).
- [4] B. Lake, G. Aeppli, T.E. Mason, A. Schroeder, D.F. McMorrow, K. Lefmann, M. Isshiki, M. Nohara, H. Takagi, and S.M. Hayden, *Nature* **400**, 43 (1999).
- [5] J.M. Tranquada, J.D. Axe, N. Ichikawa, A.R. Moodenbaugh, Y. Nakamura, and S. Uchida, *Phys. Rev. Lett.* **78**, 338 (1997).
- [6] P. Dai, H.A. Mook, and F. Dogan, *Phys. Rev. Lett.* **80**, 1738 (1998).
- [7] H.F. Fong, P. Bourges, Y. Sidis, L.P. Regnault, A. Ivanov, G.D. Gu, N. Koshizuka, and B. Keimer, *Nature* **398**, 588 (1999).
- [8] H.A. Mook, F. Dogan, and B.C. Chakoumakos, *cond-mat/9811100*.
- [9] P. Bourges, B. Keimer, L.P. Regnault, and Y. Sidis, *cond-mat/0006085*.
- [10] Y.-J. Kao, Q. Si, and K. Levin, *Phys. Rev. B* **61**, R11898 (2000).
- [11] M. Norman, *Phys. Rev. B* **61**, 14751 (2000).
- [12] K.-K. Voo and W.C. Wu, *cond-mat/9911321*.
- [13] F. Onufrieva and P. Pfeuty, *cond-mat/9903097*.
- [14] J. Brinckmann and P. Lee, *Phys. Rev. Lett.* **82**, 2915 (1999).
- [15] V. Emery and S. Kivelson, *Physica C* **235-240**, 189 (1994).
- [16] J.M. Tranquada, B.J. Sternlieb, J.D. Axe, Y. Nakamura, S. Uchida, *Nature* **375**, 561 (1995).
- [17] H. Mook and F. Dogan, *Nature* **401**, 145 (1999).
- [18] J. Ma, C. Quitmann, R.J. Kelly, P. Almeras, H. Berger, G. Margaritondo, and M. Onellion, *Phys. Rev. B* **51**, 3832 (1995).
- [19] K. Gofron, J.C. Campuzano, A.A. Abrikosov, M. Lindroos, A. Bansil, H. Ding, D. Koelling, and B. Dabrowski, *Phys. Rev. Lett.* **73**, 3302 (1994).
- [20] D.M. King, Z.-X. Shen, D.S. Dessau, D.S. Marshall, C.H. Park, W.E. Spicer, J.L. Peng, Z.Y. Li, and R.L. Greene, *Phys. Rev. Lett.* **73**, 3298 (1994).
- [21] D.S. Dessau, Z.X. Shen, D.M. King, D.S. Marshall, L.W. Lombardo, P.H. Dickinson, A.G. Loeser, J. DiCarlo, C.-H. Park, A. Kapitulnik, and W.E. Spicer, *Phys. Rev. Lett.* **71**, 2781 (1993).
- [22] K. Gofron, J.C. Campuzano, H. Ding, C. Gu, R. Liu, B. Dabrowski, B.W. Veal, W. Cramer, and G. Jennings, *J. Phys. Chem. Solids* **54**, 1193 (1993).
- [23] H.A. Mook, P. Dai, F. Dogan, and R.D. Hunt, *Nature* **404**, 729 (2000).
- [24] P.V. Bogdanov, A. Lanzara, S.A. Kellar, X.-J. Zhou, E.D. Lu, W.-J. Zheng, G. Gu, J.-I. Shimoyama, K. Kishio, H. Ikeda, R. Yoshizaki, Z. Hussain, and Z.-X. Shen, *Phys. Rev. Lett.* **85**, 2581 (2000).
- [25] We want to emphasize that the dispersion is indeed badly known because of the low resolution of ARPES measurements. Even in the long studied compound BSCCO, it was until recently that some kink in the dispersion is realised. The kink results in a reduction of velocity by a factor of 2 or more. It is interesting to note that BSCCO is a compound structurally similar to YBCO, and we actually need a v_F of YBCO several times smaller than that of LSCO.
- [26] J.P. Lu, *Phys. Rev. Lett.* **68**, 125 (1992).
- [27] A. Abrikosov, *Phys. Rev. B* **62**, 15156 (2000).
- [28] T.E. Mason, G. Aeppli, and H.A. Mook, *Phys. Rev. Lett.* **68**, 1414 (1992).
- [29] A.A. Abrikosov, *Phys. Rev. B* **57**, 8656 (1998).
- [30] V.M. Krasnov, A. Yurgens, D. Winkler, P. Delsing, and T. Claeson, *Phys. Rev. Lett.* **84**, 5860 (2000).
- [31] T. Sato, T. Yokoya, Y. Naitoh, T. Takahashi, K. Yamada, and Y. Endoh, *Phys. Rev. Lett.* **83**, 2254 (1999).
- [32] K. Gorny, O.M. Vyaselev, J.A. Martindale, V.A. Nandor, C.H. Pennington, P.C. Hammel, W.L. Hults, J.L. Smith, P.L. Kuhns, A.P. Reyes, and W.G. Moulton, *Phys. Rev. Lett.* **82**, 177 (1999).
- [33] K.-K. Voo, H.-Y. Chen, and W. C. Wu (unpublished).
- [34] J. Rendell and J. Carbotte, *Phys. Rev. B* **53**, 5889 (1996).
- [35] K.A. Kouznetsov, A.G. Sun, B. Chen, A.S. Katz, S.R. Bahcall, J. Clarke, R.C. Dynes, D.A. Gajewski, S.H. Han, M.B. Maple, J. Giapintzukis, J.-T. Kim, and D.M. Ginsberg, *Phys. Rev. Lett.* **79**, 3050 (1997).
- [36] R. Kleiner, A.S. Katz, A.G. Sun, R. Summer, D.A. Gajewski, S.H. Han, S.I. Woods, E. Dantsker, B. Chen, K. Char, M.B. Maple, R.C. Dynes, and J. Clarke, *Phys. Rev. Lett.* **76**, 2161 (1996).
- [37] A.G. Sun, D.A. Gajewski, M.B. Maple, and R.C. Dynes, *Phys. Rev. Lett.* **72**, 2267 (1994).
- [38] S. Quinlan and D. Scalapino, *Phys. Rev. B* **51**, 497 (1995).
- [39] L. Yin, S. Chakravarty, and P. W. Anderson, *Phys. Rev. Lett.* **78**, 3559 (1997).
- [40] Very recently there is a report of a comprehensive ARPES measurement on LSCO by A. Ino *et al.* in *cond-mat/0005370*. As debates on ARPES measurements frequently occur, such as the FS is hole- or electron-like in BSCCO [see P.V. Bogdanov *et al.*, *cond-mat/0005394*, and references therein], and the existence or not of an extended-vHS in Sr_2RuO_4 [see A.V. Puchkov *et al.*, *Phys. Rev. B* **58**, R13322 (1998), and references therein], we think that it is still early to discuss the effect of the result by A. Ino *et al.* on our conclusion.
- [41] A.V. Chubukov, B. Janko, and O. Tchernyshyov, *cond-mat/0012065*.
- [42] D.S. Marshall, D.S. Dessau, A.G. Loeser, C.-H. Park, A.Y. Matsuura, J.N. Eckstein, I. Bozovic, P. Fournier, A. Kapitulnik, W.E. Spicer, and Z.-X. Shen, *Phys. Rev. Lett.* **76**, 4841 (1996).